

Time-Varying, Frequency-Domain Modeling and Analysis of Phase-Locked Loops with Sampling Phase-Frequency Detectors

Piet Vanassche, Georges Gielen and Willy Sansen
Katholieke Universiteit Leuven - ESAT/MICAS
<http://www.esat.kuleuven.ac.be/micas/>

Abstract

This paper presents a new, frequency-domain based method for modeling and analysis of phase-locked loop (PLL) small-signal behavior, including time-varying aspects. Focus is given to PLLs with sampling phase-frequency detectors (PFDs) which compute the phase error only once per period of the reference signal. Using the harmonic transfer matrix (HTM) formalism, the well-known continuous-time, linear time-invariant (LTI) approximations are extended to take the impact of time-varying behavior, arising from the sampling nature of the PFD, into account. Especially for PLLs with a fast feedback loop, this time-varying behavior has severe impact on, for example, loop stability and cannot be neglected. Contrary to LTI analysis, our method is able to predict and quantify these difficulties. The method is verified for a typical loop design.

1. Introduction

Phase-locked loops (PLLs) are used in both analog and digital systems for generating signals that track the phase of a given reference signal. They can be used to reduce oscillator phase noise by phase-locking it to a high-quality reference, to synthesize frequencies which are multiples of the input frequency or, in digital applications, to buffer and deskew clock signals. In a lot of applications, PLLs are among those blocks whose performance is crucial in meeting system-level specifications. Adequate analysis of their behavior is therefore of great importance.

A typical PLL architecture, illustrated in Fig. 1, consists of a voltage controlled oscillator (VCO)¹, a phase-frequency detector (PFD) and a loop filter $H_{LF}(s)$. Nowadays, one most commonly uses digital PFDs which steer a charge-pump [7], this because of their superior acquisition of phase-lock. These PFDs measure the phase error

¹In this text, we assume prescalers to be included in the VCO models.

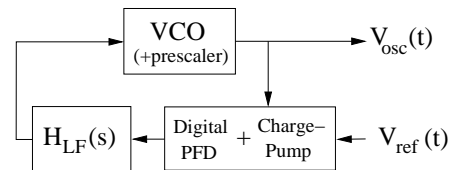


Figure 1. Typical PLL architecture.

as the distance between the zero-crossings of the reference signal and the VCO signal. Therefore, they only compute the phase error once per period of the reference signal, i.e. they sample the phase error. For this reason, we call them *sampling PFDs*. Due to their sampling nature, these PFDs introduce linear periodically time-varying (LPTV) components in the PLL's small-signal behavior. So, in analyzing a PLL, we are essentially dealing with a periodically time-varying system, as opposed to a time-invariant one, e.g. a filter. Especially for PLLs with a fast feedback loop, this time-varying behavior has severe impact on, for example, loop stability and cannot be neglected.

This paper introduces a method to deal with the time-varying aspects of a PLL's small-signal behavior using a frequency-domain description grounded on the harmonic transfer matrix (HTM) formalism [9, 10]. This approach is able to predict and quantify the difficulties that arise in PLLs due to their time-varying nature. Furthermore, being a frequency-domain description, it allows us to recover powerful tools and concepts from the theory of LTI systems, like transfer functions and phase margin, for analyzing PLL time-varying behavior.

Classical textbook analyses typically model PLL small-signal behavior using continuous-time, linear time-invariant (LTI) feedback theory [2, 7]. This approximation works fine as long as the unity gain frequency of the feedback loop is well below the frequency of the reference signal. If this condition no longer holds, the approximation runs into trouble. Especially for PLLs with a fast feedback loop and a sampling PFD, the impact of time-varying behavior on system performance can become quite dramatic. For

this case, [3, 5] suggest to treat PLLs as discrete-time systems. This analysis reveals constraints on the design of a PLL's open-loop characteristic that are not readily derived using continuous-time approximations. However, using z -domain models, [3, 5] still don't fully recognize the mixed continuous-time/discrete-time nature of PLLs. Furthermore, they are not very well suited as a framework for symbolic computations, at least not for arbitrary loop characteristics. This limits their help in gaining understanding and making decisions on design parameters.

This work presents a method for constructing s -domain PLL small-signal models that include the time-varying aspects of PLL behavior. Although extension to arbitrary PFDs is possible, this work focuses on PLLs using sampling PFDs since those occur most commonly. The model is stated in terms of the HTM formalism [9, 10]. It is a frequency-domain approach, extending ideas and intuitions on LTI systems to include a PLL's time-varying behavior. Furthermore, this method can be used to obtain both numerical results and symbolic expressions.

The remainder of this article is structured as follows. Section 2 provides a brief summary on HTMs. Next, section 3 discusses how to model the behavior of the PLL building blocks in terms of these HTMs. In section 4, the building block models are connected in order to obtain the input-output HTM of the overall PLL. Experimental results are presented in section 5. Finally, section 6 draws some conclusions.

2. A brief summary on HTMs

Considering a general LPTV system, its input-output relation is described by

$$y(t) = H[u(t)] = \int_{-\infty}^{\infty} h(t, \tau)u(t - \tau)d\tau . \quad (1)$$

Here, $u(t)$ is the input, $y(t)$ is the output and $h(t, \tau)$ is the kernel describing the system's behavior. Since for LPTV systems, the kernel $h(t, \tau)$ is T -periodic in the variable t , it can be expanded as a Fourier series with respect to t . This yields

$$y(t) = \sum_{k=-\infty}^{+\infty} e^{jk\omega_0 t} \int_{-\infty}^{+\infty} h_k(\tau)u(t - \tau)d\tau , \quad (2)$$

with $\omega_0 = 2\pi/T$. The functions $h_k(\tau)$ are called the harmonic impulse responses and their Laplace transforms

$$H_k(s) = \mathcal{L}\{h_k(\tau)\} \quad (3)$$

the harmonic transfer functions. Introducing the ∞ -dimensional vector

$$\tilde{\mathbf{U}}(s) = \left[\cdots \quad U(s - j\omega_0) \quad U(s) \quad U(s + j\omega_0) \quad \cdots \right]^T \quad (4)$$

—with similar definition for $\tilde{\mathbf{Y}}(s)$ — and the infinite-dimensional matrix $\tilde{\mathbf{H}}(s)$ with elements

$$\tilde{H}_{n,m}(s) = H_{n-m}(s + jm\omega_0) , \quad (5)$$

it can be shown that the input-output relation (1) has the frequency-domain equivalent

$$\tilde{\mathbf{Y}}(s) = \tilde{\mathbf{H}}(s)\tilde{\mathbf{U}}(s) . \quad (6)$$

The matrix $\tilde{\mathbf{H}}(s)$ is called the harmonic transfer matrix (HTM) [9, 10] corresponding to the LPTV system (1). When truncated and evaluated at $s = j\omega$, it corresponds to the harmonic conversion matrix as introduced in [8].

The nature of the HTM-representation is clarified by considering the input-output behavior for

$$u(t) = \sum_{m=-\infty}^{+\infty} u_m(t)e^{jm\omega_0 t} . \quad (7)$$

Here, the $u_m(t)$ have Fourier spectra $U_m(j\omega) = \mathcal{F}\{u_m(t)\}$, band-limited within $[-\omega_0/2, \omega_0/2]$. They hence model the signal content around the carriers at $\omega = m\omega_0$. Defining

$$\tilde{\mathbf{U}}_B(j\omega) = \left[\cdots \quad U_{-1}(j\omega) \quad U_0(j\omega) \quad U_1(j\omega) \quad \cdots \right]^T \quad (8)$$

as the vector containing the input signal's equivalent base-band components, then, with a similar definition for $\tilde{\mathbf{Y}}_B(s)$, it can be shown that

$$\tilde{\mathbf{Y}}_B(j\omega) = \tilde{\mathbf{H}}(j\omega)\tilde{\mathbf{U}}_B(j\omega) . \quad (9)$$

This implies that the matrix element $\tilde{H}_{n,m}(j\omega)$ characterizes the transfer of the signal content from the input signal frequency band around $m\omega_0$ to the output signal frequency band around $n\omega_0$. In short, $\tilde{\mathbf{H}}(s)$ characterizes how information moves from one frequency-band to another. This process is illustrated in Fig. 2.

Besides offering an elegant frequency-domain characterization of LPTV behavior, HTMs also provide an efficient way to manipulate LPTV systems and to compute the overall input-output behavior, given the system's building block models. The HTMs corresponding respectively to the parallel connection $y = H_1[u] + H_2[u]$ and the series connection $y = H_2[H_1[u]]$ are given by

$$\tilde{\mathbf{H}}_+(s) = \tilde{\mathbf{H}}_1(s) + \tilde{\mathbf{H}}_2(s) \quad (10)$$

$$\tilde{\mathbf{H}}_\times(s) = \tilde{\mathbf{H}}_2(s)\tilde{\mathbf{H}}_1(s) . \quad (11)$$

Furthermore, HTMs corresponding to basic building block systems are computed in a straightforward manner. An LTI system with transfer function $H(s)$ corresponds to the HTM whose elements are given by

$$\begin{cases} \tilde{H}_{n,m}(s) = H(s + jm\omega_0) & m = n \\ \tilde{H}_{n,m}(s) = 0 & m \neq n \end{cases} , \quad (12)$$

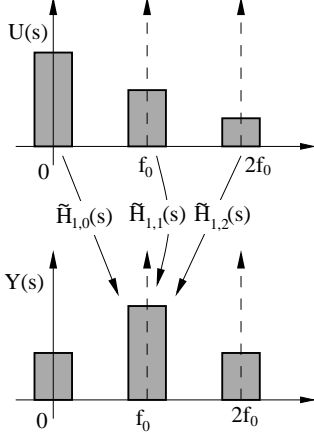


Figure 2. Signal transfers between the different input and output frequency bands.

Note this HTM having a diagonal structure. On the other hand, the elements of the HTM corresponding to the memoryless multiplication $y(t) = p(t)u(t)$, with $p(t) = \sum_{k=-\infty}^{+\infty} P_k e^{jk\omega_0 t}$, are specified by

$$\tilde{H}_{n,m}(s) = P_{n-m} \quad (13)$$

Using (10)-(13), HTMs corresponding to more complex systems can be determined from their topology and building block HTMs.

3. Modeling the PLL building blocks

In constructing the HTM describing a PLL's overall input-output behavior, we first need to determine the HTMs corresponding to the building blocks in Fig. 1. The next couple of sections respectively describe the PFD, loop filter and VCO models together with the HTMs that accompany them. Note that when talking about the phase θ_{ref} of the reference signal and the phase θ of the VCO, these are related to the signal models

$$V_{ref}(t) = x_{ref}(t + \theta_{ref}(t)) \quad (14)$$

$$V_{osc}(t) = x_{osc}(t + \theta(t)) \quad (15)$$

where both $x_{ref}(t)$ and $x_{osc}(t)$ are T -periodic waveforms. In what follows, we furthermore assume $|\theta_{ref}/T| \ll 1$, i.e. it represents a small-signal excursion. In a stable PLL that has acquired phase-lock, this implies that $|\theta/T| \ll 1$.

3.1. Sampling phase-frequency detector

In sampling PFDs, the phase error $\theta_{ref} - \theta$ between the reference and VCO output is measured (sampled) once per

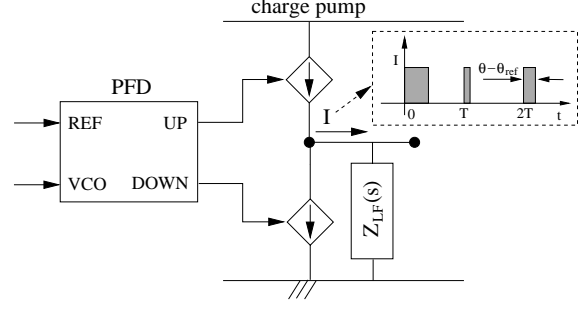


Figure 3. Sampling phase-frequency detector. The reference and VCO phase are compared using sequential digital logic which steers a charge pump. The impedance $Z_{LF}(s)$ acts as the loop filter.

period of the reference signal. Typical sampling circuits, like the charge pump based topology in Fig. 3 [7], code this error as the width of a sequence of digital pulses. If the width of these pulses is small compared to the time-constant of the loop filter–VCO combination, they will have the same effect as Dirac impulses with their weight equal to the width of the original pulses. This equivalence is depicted in Fig. 4. Note that the pulses in the upper plot were normalized to have magnitude 1. The effective charge-pump current I_{cp} will be taken into account in the loop filter model.

Assuming the equivalence in Fig. 4 to hold, the input-output relation of a sampling PFD can be modeled as a multiplication of the phase error $\theta_{ref} - \theta$ with a Dirac impulse train, or

$$y(t) = \left(\sum_{m=-\infty}^{+\infty} \delta(t - mT) \right) (\theta_{ref}(t) - \theta(t)) \quad (16)$$

$$= \frac{\omega_0}{2\pi} \left(\sum_{m=-\infty}^{+\infty} e^{jm\omega_0 t} \right) (\theta_{ref}(t) - \theta(t)) \quad (17)$$

with $T = 2\pi/\omega_0$ the sampling period. Using (13), this multiplication can be stated in terms of HTMs as

$$\tilde{Y}(s) = \tilde{\mathbf{H}}_{PFD}(s) \left(\tilde{\theta}(s) - \tilde{\theta}_{ref}(s) \right) \quad (18)$$

with

$$\tilde{\mathbf{H}}_{PFD}(s) = \frac{\omega_0}{2\pi} \begin{bmatrix} \vdots & \vdots & \vdots & \vdots \\ \cdots & 1 & 1 & 1 & \cdots \\ \cdots & 1 & 1 & 1 & \cdots \\ \cdots & 1 & 1 & 1 & \cdots \\ \vdots & \vdots & \vdots & \vdots & \vdots \end{bmatrix} \quad (19)$$

$$= \frac{\omega_0}{2\pi} \mathbf{1} \cdot \mathbf{1}^T \quad (20)$$

relating changes in the reference phase to changes in the VCO phase.

Considering the fact that elaborating (28) involves the inversion of an, in principle, ∞ -dimensional matrix, this expression does not seem to hold much practical value. However, by exploiting the fact that $\tilde{\mathbf{H}}_{PFD}(s) = (\omega_0/2\pi) \mathbf{I} \cdot \mathbf{I}^T$ is of rank one, it is possible to obtain a closed-form expression for $(\mathbf{I} + \tilde{\mathbf{G}}(s))^{-1}$, and hence for the input-output relation (28). Defining

$$\tilde{\mathbf{V}}(s) = \frac{\omega_0}{2\pi} \tilde{\mathbf{H}}_{VCO}(s) \cdot \tilde{\mathbf{H}}_{LF}(s) \cdot \mathbf{1}, \quad (29)$$

we can write

$$\tilde{\mathbf{G}}(s) = \tilde{\mathbf{V}}(s) \cdot \mathbf{I}^T. \quad (30)$$

Using the Sherman-Morrisson-Woodbury formula [4], we then find

$$(\mathbf{I} + \tilde{\mathbf{G}}(s))^{-1} = (\mathbf{I} + \tilde{\mathbf{V}}(s) \cdot \mathbf{I}^T)^{-1} \quad (31)$$

$$= \mathbf{I} - \frac{\tilde{\mathbf{V}}(s) \cdot \mathbf{I}^T}{1 + \lambda(s)} \quad (32)$$

with

$$\lambda(s) = \mathbf{I}^T \tilde{\mathbf{V}}(s) = \mathbf{I}^T [\tilde{\mathbf{H}}_{VCO}(s) \cdot \tilde{\mathbf{H}}_{LF}(s)] \mathbf{1}. \quad (33)$$

In words, $\lambda(s)$ equals the sum of all elements of $\tilde{\mathbf{H}}_{VCO}(s) \cdot \tilde{\mathbf{H}}_{LF}(s)$. Substituting (32) in (28) and using (30), the input-output relation becomes

$$\tilde{\theta}(s) = \left(\frac{1}{1 + \lambda(s)} \tilde{\mathbf{V}}(s) \cdot \mathbf{I}^T \right) \tilde{\theta}_{ref}(s). \quad (34)$$

This relation is straightforward to evaluate numerically. It can also be used as a starting point for obtaining symbolic results.

5. Experimental results

We illustrate and verify our method for PLL loops with time-invariant VCO behavior. Computations obtained using the HTM framework are compared with results from time-marching simulations in Matlab/SimulinkTM. The Matlab/Simulink model implements the PFD using flip-flops and therefore encodes the phase error through the width of the pulses it produces. This corresponds to the behavior of an actual circuit realization. It allows us to test the accuracy of our approximations.

Time-invariance of the VCO implies that in (25), $v_k = 0, \forall k \neq 0$. The HTM becomes diagonal and represents an LTI system with transfer characteristic $H_{VCO}(s) = v_0/s$. The open-loop gain of the continuous-time LTI approximation then becomes

$$A(s) = \frac{\omega_0 v_0}{2\pi s} H_{LF}(s). \quad (35)$$

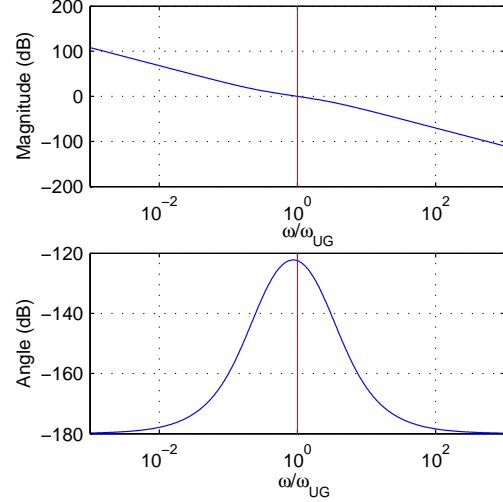


Figure 5. Typical characteristic for $A(j\omega)$.

The factor $\omega_0/2\pi$ in front arises from the sampling PFD model (19). Fig. 5 shows a typical gain characteristic. It contains three poles (the first two at DC) and one zero. Note that the frequency-axis is normalized with respect to the unity-gain frequency ω_{UG} of $A(s)$. This characteristic will be used for further numerical computations.

Using (33) and (34), the input-output HTM $\tilde{\mathbf{H}}(s)$ is found to equal

$$\tilde{\mathbf{H}}(s) = \frac{1}{1 + \lambda(s)} \begin{bmatrix} \vdots \\ A(s - j\omega_0) \\ A(s) \\ A(s + j\omega_0) \\ \vdots \end{bmatrix} \begin{bmatrix} \cdots & 1 & 1 & 1 & \cdots \end{bmatrix} \quad (36)$$

with

$$\lambda(s) = \sum_{m=-\infty}^{+\infty} A(s + jm\omega_0) \quad (37)$$

being the effective open-loop gain. The HTM element $\tilde{H}_{0,0}(s)$, modeling the closed-loop signal transfers from baseband to baseband, is given by

$$\tilde{H}_{0,0}(s) = \frac{A(s)}{1 + \lambda(s)} \approx \frac{A(s)}{1 + A(s)}. \quad (38)$$

The latter approximation, corresponding to classical LTI analysis, is valid as long as $|A(s)| \gg \left| \sum_{m \neq 0} A(s + jm\omega_0) \right|$. If this no longer holds, i.e. when time-varying effects become important, the other terms of $\lambda(s)$ need to be taken into account. This is the case as the frequency range of interest, characterized by the unity gain frequency ω_{UG} of $A(s)$, approaches ω_0 . Note that signal

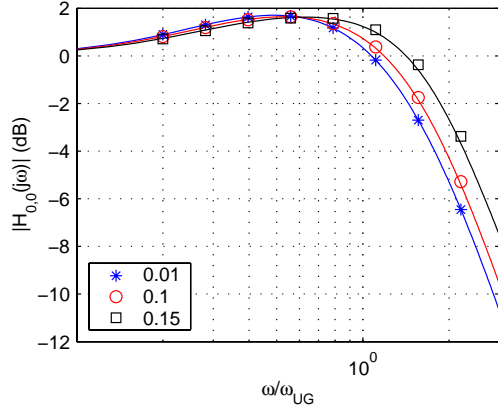


Figure 6. Baseband to baseband signal transfer, represented by the HTM element $\tilde{H}_{0,0}(s)$, for $\omega_{UG}/\omega_0 = 0.01, 0.1$ and 0.15 .

transfers to other frequency bands can be studied as well by considering the other elements of $\tilde{\mathbf{H}}(s)$.

Fig. 6 shows the impact of an increasing ω_{UG}/ω_0 on $\tilde{H}_{0,0}(s)$. The solid lines are obtained by evaluating (38) while the marks are extracted from time-marching simulations. Both are within 2%. Note, however, that evaluating (38) is only a matter of seconds while it takes several minutes for the time-marching simulations to complete.

Observing $\tilde{H}_{0,0}(s)$, it is seen that the effective bandwidth shifts to the right as ω_{UG}/ω_0 increases. Also, peaking at the passband's edge becomes worse. Fig. 7 explains this behavior in terms of the effective open-loop gain $\lambda(s)$. The increase of the closed-loop bandwidth corresponds to the increase of $\omega_{UG,eff}$, the unity gain frequency of $\lambda(s)$. More important is the phase margin of $\lambda(s)$ which is rapidly degrading for increasing ω_{UG}/ω_0 . For $\omega_{UG}/\omega_0 = 0.1$, this phase margin is already 9% worse than predicted by LTI analysis. This clearly illustrates the need to take time-varying effects into account for proper design of a PLL's behavior.

6. Conclusions

Time-varying effects, especially for PLLs implemented with a fast feedback loop and a sampling PFD, have a significant impact on PLL system performance and cannot be neglected. This paper has presented a method to deal with the time-varying aspects of a PLL's small-signal behavior using a frequency-domain description grounded on the HTM formalism. This approach is able to predict and quantify the difficulties, e.g. degrading loop stability, that arise in PLLs due their time-varying nature. Furthermore, being a frequency-domain description, it allows us to recover pow-

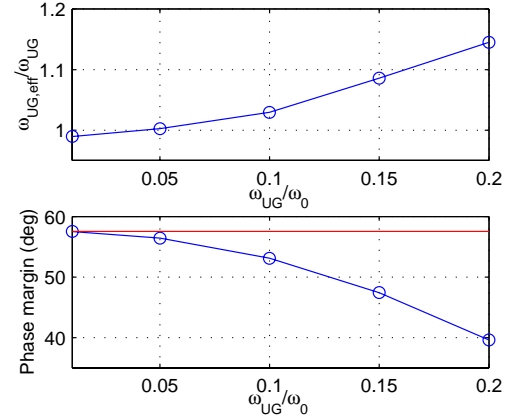


Figure 7. The normalized effective unity gain frequency $\omega_{UG,eff}/\omega_{UG}$ (upper plot) and the open loop phase margin (lower plot) versus ω_{UG}/ω_0 . The horizontal line indicates the phase margin as predicted by LTI analysis.

erful tools and concepts from the theory of LTI systems, like transfer functions and phase margin, for analyzing PLL time-varying behavior. The method can be used to obtain both numerical results and symbolic expressions.

References

- [1] A. Demir, A. Mehrotra and J. Roychowdhury, "Phase Noise in Oscillators: A Unifying Theory and Numerical Methods for Characterization", In *IEEE Trans. Circ. and Syst.-I*, vol. 47, no. 5, pp. 655-674, May 2000
- [2] F.M. Gardner, *Phaselock Techniques*, 2nd. ed., John Wiley & Sons Inc., 1979
- [3] F.M. Gardner, "Charge-Pump Phase-Lock Loops", In *IEEE Trans. Communications*, vol. com-28, no. 11, November 1980
- [4] G.H. Golub and C.F. Van Loan, *Matrix Computations*, 3rd edition, The John Hopkins University Press, 1996
- [5] J.P. Hein and J.W. Scott, "z-Domain Model for Discrete-Time PLL's", In *IEEE Trans. Circuits and Systems*, vol. 35, no. 11, November 1988
- [6] V. Hutson and J.S. Pym, *Applications of Functional Analysis and Operator Theory*, Math. in Science and Engineering, vol. 146, Academic Press, 1980
- [7] T.H. Lee, *The design of CMOS radio-frequency integrated circuits*, Cambridge University Press, 1998
- [8] S.A. Maas, *Nonlinear microwave circuits*, Norwood: Artech House, 1988
- [9] E. Möllerstedt and B. Bernhardsson, "Out of Control Because of Harmonics", In *IEEE Control Systems Magazine*, pp. 70-81, 2000
- [10] P. Vanassche, G. Gielen and W. Sansen, "Symbolic modeling of periodically time-varying systems using harmonic transfer matrices", In *IEEE Trans. on Computer-Aided Design*, vol. 21, nr. 9, September 2002